

# Use of susceptibility weighted imaging to assess hemorrhage in brain metastases

Feride Kural Rahatli, Fuldem Yildirim Donmez, Kemal Murat Haberal, Ahmet Muhtesem Agildere

Baskent University, Faculty of Medicine, Department of Radiology, Ankara, Turkey

Copyright © 2018 by authors and Annals of Medical Research Publishing Inc.

## Abstract

**Aim:** Detection of intratumoral hemorrhage in metastatic lesions leads to determination of treatment options. We evaluated the diagnostic value of precontrast SWI for the detection of blood products in brain metastases by comparing SWI to conventional sequences.

**Material and Methods:** Brain magnetic resonance imaging (MRI) sequences were acquired between April 2014 and November 2015 from 21 patients with brain metastases, and were retrospectively evaluated for the presence of hemorrhagic elements. All examinations were performed on a 1.5 Tesla Siemens scanner. Our routine protocol included axial T1-weighted (T1W), T2-weighted (T2W), and FLAIR sequences, coronal and sagittal T2W sequences, post gadolinium axial and sagittal T1W sequences, and a coronal FSE T1W sequence, in addition to the precontrast SWI sequence.

**Results:** Seventy-one intraparenchymal metastatic lesions (range: 0.5–3.5 cm) were detected. No hemorrhages were detected in 25 lesions (35.2%), while in 12 lesions (16.9%) hemorrhage was detected by SWI and T1 and/or T2 weighted images. In 34 lesions (47.88%) hemorrhage was detected only on the SWI sequence, and it was not seen on the conventional sequences.

**Conclusion:** SWI provided better information for the evaluation of intratumoral hemorrhage than T1W and T2W sequences of the inner structure of metastases. T1W and T2W images did not provide sufficient detection of hemorrhagic elements; SWI is therefore needed to detect intratumoral hemorrhage, and the sequence should be added to the protocol to allow better characterization.

**Keywords:** Metastasis; Brain; Susceptibility weighted imaging; Hemorrhage.

## INTRODUCTION

Susceptibility-weighted imaging (SWI) using a three-dimensional (3D) high-resolution fully flow-compensated gradient echo sequence (GRE) combines the information from both magnitude and phase images to exploit the magnetic susceptibility differences of tissue contents such as blood, iron, and calcium (1,2). SWI provides supplementary information on hemorrhage, venous vasculature, vascular malformations, and calcification in the brain (3,4).

Deoxyhemoglobin shows a markedly hypointense signal on SWI; however, during the evolution of hemorrhage, the signal on SWI images increases because of the destruction of red blood cells, while in the chronic stage of hemorrhage, a reduced signal is seen owing to the presence of hemosiderin and ferritin (5).

Several studies have compared SWI to conventional magnetic resonance imaging (MRI) sequences, and

these have demonstrated the value of SWI sequences for the detection of microhemorrhages and vasculature in primary brain tumors (6,7). Hemorrhage is seen mostly in high grade brain tumors. Detecting micro hemorrhage in primary brain tumors could be helpful in tumor staging and treatment choices (6).

Aggressive metastatic tumors grow rapidly and incline to have high vascularity and microhemorrhage. Intratumoral hemorrhage detection in metastatic brain tumors can lead to determination of treatment choices. It has been shown that hemorrhage in melanoma metastasis could have negative prognostic effect (8,9).

Intratumoral hemorrhage is frequently seen in both primary brain tumors and metastases, with histopathological studies having reported an incidence of 36% in brain metastases, 30% in oligodendrogliomas, and 13% in glioblastoma (10).

The purpose of this study was therefore to evaluate the

**Received:** 22.01.2018 **Accepted:** 26.04.2018 **Available online:** 08.10.2018

**Corresponding Author:** Feride Kural Rahatli, Baskent University, Faculty of Medicine, Department of Radiology, Ankara, Turkey  
E-mail: drkural@hotmail.com

diagnostic value of precontrast SWI for the detection of hemorrhage in brain metastases, making comparisons with conventional sequences.

## MATERIAL and METHODS

### Patients

This study was performed in accordance with the ethical guidelines of the Declaration of Helsinki and was approved by the ethics committee of the university. Brain MRI sequences from 21 cancer patients with brain metastases that were treated at our hospital between April 2014 and November 2015 were analyzed retrospectively.

Metastatic brain tumors were diagnosed on the basis of clinical information indicative of systemic metastatic tumors and evidence of multiple mass lesions on conventional brain MRI and follow-up brain MRIs.

None of the patients had a history of cranial biopsy or surgery. Among these 21 patients, the primary diagnoses were non-small cell lung carcinoma (n = 11), small cell lung carcinoma (n = 1), renal cell carcinoma (n = 1), bladder transitional cell carcinoma (n = 1), pancreas adenocarcinoma (n = 1), ovarian carcinoma (n = 1), colorectal adenocarcinoma (n = 2), invasive breast carcinoma (n = 2), and gastric adenocarcinoma (n = 1).

### Magnetic Resonance Imaging

All MRI studies were performed on a 1.5 T MRI scanner (Avanto, Siemens Medical Solutions, Erlangen, Germany) with a 16-channel phased array head coil. The imaging protocol consisted of axial SWI (TR/TE: 50/40 ms; slice thickness: 2.5 mm; field of view (FOV): 22 cm; matrix size: 256 × 320; FA: 15°) axial FLAIR images (TR/TE: 8000/84 ms; slice thickness: 5.5 mm; FOV: 22 cm; matrix size: 256 × 157; bandwidth: 190; flip angle: 150°; number of slices: 20), axial T1-weighted images (TR/TE: 410/9.2 ms; slice thickness: 5.5 mm; FOV: 22 cm; matrix size: 448 × 186; bandwidth: 130; flip angle: 90°; number of slices: 20), axial T2-weighted images (TR/TE: 3630/103 ms; slice thickness: 5.5 mm; FOV: 22 cm; matrix size: 512 × 325; bandwidth: 191; flip angle: 150°; number of slices: 20), coronal T2-weighted images (TR/TE: 3630/103 ms; slice thickness: 5.5 mm; FOV: 22 cm; matrix size: 512 × 302; bandwidth: 191; flip angle: 150°; number of slices: 20), sagittal T2-weighted images (TR/TE: 3630/103 ms; slice thickness: 5.5 mm; FOV: 22 cm; matrix size: 512 × 358; bandwidth: 191; flip angle: 150°; number of slices: 20), post-gadolinium-enhanced axial and sagittal T1-weighted images, and coronal fat-suppressed T1-weighted images (TR/TE: 552/17 ms; slice thickness: 5.5 mm; FOV: 22 cm; matrix size: 384 × 192; bandwidth: 130; flip angle: 90°; number of slices: 20). A standard dose of gadobenate-dimeglumine (Multihance) at 0.1 mmol or 0.2 ml/kg was intravenously delivered as a bolus.

The total imaging time for the cranial MRI was nearly 20 minutes.

### Image analysis

MR scans were visually evaluated by two neuroradiologists with 6 and 10 years of experience in neuroradiology, with the SWI sequences being compared with the conventional sequences on a slice by slice basis. The SWI sequences were used to detect intratumoral dot-like or linear hypointense signal changes, with the phase images being used to exclude calcification (11).

Tumors were measured on post-gadolinium-enhanced T1-weighted images according to the RANO criteria (12).

## RESULTS

The cranial MRI sequences of 21 (10 males and 11 females) patients with metastatic brain tumors were retrospectively evaluated for the presence of hemorrhage. Patients were aged between 49 and 86 years, with a median age of 64 years. Seventy-one intraparenchymal metastatic lesions ranging from 0.5 to 35 mm were detected, with the number of lesions per patient ranging from two to 13.

In 25 lesions (35.2%), no hemorrhage was detected on conventional T1- and T2-weighted sequences, or on the SWI sequence. In 12 lesions (16.9%), hemorrhage was detected on either or both of the T1- and T2-weighted images, and also on the SWI. In one of these 12 lesions, hemorrhage was evident only on the T1-weighted images as a hyperintense area, while in two of the lesions, hemorrhages were detected only on the T2-weighted images as hypointense areas. In nine of the 12 lesions, hemorrhage was detected on both T1 and T2 weighted images (Figure 1).

In 34 lesions (47.88%), hemorrhages were observed only on the SWI sequences, as hypointense areas that were not observed on the conventional sequences (Figure 2).

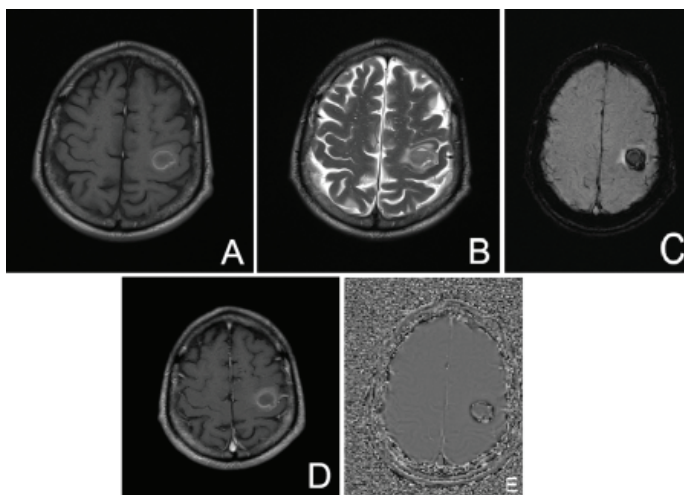


**Figure 1.** A 62-year-old male patient with metastatic non-small cell lung carcinoma. A left parietal solid mass is hypointense on axial T1-weighted imaging (a), but minimally hyperintense on axial T2-weighted imaging (b). A hyperintense rim representing hemorrhage is visible on both T1- and T2-weighted imaging. Hemorrhage is more prominent on the axial SWI sequence (c). On axial postcontrast T1-weighted imaging (d), the lesion demonstrates peripheral enhancement. (e) Phase images showing hemorrhage as hyperintense areas.

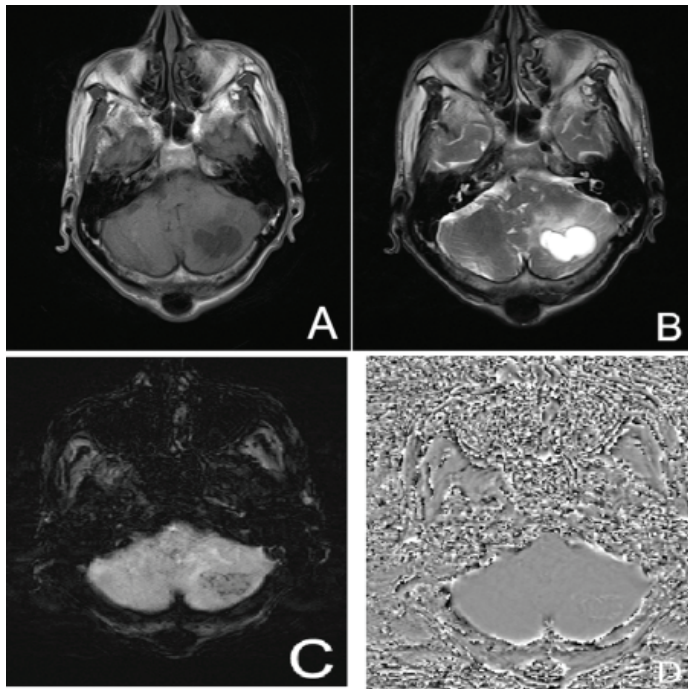


**Figure 2.** A 68-year-old male patient with metastatic gastric adenocarcinoma. A left cerebellar cystic mass is hypointense on axial T1-weighted imaging (a), and hyperintense on axial T2-weighted imaging (b), with no evidence of hemorrhage visible on either T1- or T2-weighted imaging. On the axial SWI sequence (c), dot shaped hypointensities representing hemorrhage are visible. (d) phase images showing hemorrhage as hyperintense areas.

## DISCUSSION

The major conclusion of our study is that SWI provided better information for the detection of intratumoral hemorrhages in brain metastases than did T1- and T2-weighted sequences. In the current study, the phase images from the SWI were used to differentiate calcification from hemorrhage (Figure 1,2). Diamagnetic calcium, which is hypointense on SWI, shows a negative phase and remains hypointense on the phase images. Deoxyhemoglobin in a hemorrhage, which is hypointense on SWI, shows a positive phase and is hyperintense on the phase images (5). Computed tomography (CT) could also be used to differentiate calcification from hemorrhage. Berberat et al evaluated 11 patients with gliomas and compared the value of CT and SWI phase images in the detection of intratumoral hemorrhage (13). They found that phase images allowed correct differentiation between calcification and hemorrhage in 86% of cases.

Sehgal et al evaluated 44 patients with primary brain tumors and metastases and compared SWI sequence to conventional sequences (2). They found that SWI was superior to T1- and T2-weighted sequences for the detection of blood products. Hori et al (3) found that SWI was helpful in the visualization of tumoral architecture and characteristics. Zhang et al found SWI superior to T1- and T2-weighted sequences in detection of intratumoral hemorrhage lung cancer patients with brain metastasis (14) Pinker et al demonstrated intratumoral susceptibility

effects in both pre- and post-contrast SWI images, together with contrast enhancement in both post-contrast SWI and T1-weighted images of 19 patients with primary brain tumors (6). In the current study, we did not perform a post-contrast axial SWI sequence, and thus we did not evaluate tumoral enhancement on the SWI sequence. Our findings on the evaluation of intratumoral hemorrhage are similar to those described in the literature.

Roelke et al assessed 105 patients with newly diagnosed brain metastases and glial tumors, with an axial SWI sequence being acquired in addition to the conventional sequences (15). They found that detection of intratumoral hemorrhage was more frequent than indicated by histopathological analysis, which they explained as being a result of insufficient specimen on biopsy or partial resection. Kondziolka et al performed clinical and histopathological evaluations of 905 patients with brain tumors and reported an incidence of hemorrhage of 36% in brain metastases, 30% in oligodendrogliomas, and 13% in glioblastoma (10). In this study patients did not go craniotomy; the diagnosis of intratumoral hemorrhage was based on SWI findings. We did not correlate histopathological analysis and SWI findings, but in our study incidence of intratumoral hemorrhage was higher than the previous histopathological study.

Pinker et al evaluated patients with primary brain tumors and reported that SWI was useful for grading gliomas (6). They found a correlation between the frequency of intratumoral susceptibility effects and the tumor grade. It is known that high grade glial tumors contain a large quantity of blood products, which can be explained by the increased blood supply and prominent angiogenesis. These blood products produce susceptibility effects and cause hypointense areas on SWI. Aggressive metastatic tumors grow rapidly incline to have high vascularity and microhemorrhage. Presence of intratumoral hemorrhage with clinico pathological and other radiological findings is important in prognosis and treatment decision in brain metastasis (8). Intratumoral hemorrhage detection in metastatic brain tumors can lead to determination of treatment choices. It has been shown that low intratumoral hemorrhage was associated with prolonged overall survival in melanoma patients with brain metastasis (9).

Park et al found that an SWI sequence could be used for grading gliomas on 3 T MRI, but thought that the clinical use of an SWI sequence on 1.5 T MRI was limited because of the long scan times (16). However, Sehgal et al and Hori et al studied patients with brain tumors on 1.5 T MRI, and they suggested that SWI could be available on 1.5 T MRI in clinical use. In our opinion, an SWI sequence on 1.5 T MRI is useful for evaluating brain tumors. Although most of our patients had a poor clinical condition because of their primary diseases, they tolerated MRI very well, and the SWI sequences were free of any motion artifacts.

Our study is limited by the relatively small sample size and the absence of histopathological and CT correlations. However, we did use the phase images to rule out the presence of calcification.

## CONCLUSION

SWI provided better information for the evaluation of intratumoral hemorrhage than T1- and T2-weighted sequences. T1-weighted T2-weighted sequences are inferior to SWI sequence showing intratumoral hemorrhage so SWI should be added to the MRI protocol to show microhemorrhage and better characterize the inner structure of metastases. Further studies with a larger sample size should be performed, and these should take the association between clinical symptoms and intratumoral hemorrhage into consideration.

*Competing interests: The authors declare that they have no competing interest.*

*Financial Disclosure: There are no financial supports*

*Ethical approval: This work has been approved by the Institutional Review Board.*

## REFERENCES

1. Reichenbach JR, Venkatesan R, Schillinger DJ, Kido DK, Haacke EM. Small vessels in the human brain: MR venography with deoxyhemoglobin as an intrinsic contrast agent. *Radiology* 1997;204(1):272-7.
2. Sehgal V, Delproposto Z, Haddar D, Haacke EM, Sloan AE, Zamorano LJ, et al. Susceptibility-weighted imaging to visualize blood products and improve tumor contrast in the study of brain masses. *J Magn Reson Imaging* 2006;24(1):41-51.
3. Hori M, Ishigame K, Kabasawa H, Kumagai H, Ikenaga S, Shiraga N, et al. Precontrast and postcontrast susceptibility-weighted imaging in the assessment of intracranial brain neoplasms at 1.5 T. *Jpn J Radiol* 2010;28(4):299-304.
4. Rauscher A, Sedlacik J, Barth M, Mentzel HJ, Reichenbach JR. Magnetic susceptibility-weighted MR phase imaging of the human brain. *AJNR Am J Neuroradiol* 2005;26(4):736-42.
5. Gomori JM, Grossman RI, Yu-Ip C, Asakura T. NMR relaxation times of blood: dependence on field strength, oxidation state, and cell integrity. *J Comput Assist Tomogr* 1987;11(4):684-90.
6. Pinker K, Noebauer-Huhmann IM, Stavrou I, Hoeffberger R, Szomolanyi P, Weber M, et al. High-field, high-resolution, susceptibility-weighted magnetic resonance imaging: improved image quality by addition of contrast agent and higher field strength in patients with brain tumors. *Neuroradiology* 2008;50(1):9-16.
7. Pinker K, Noebauer-Huhmann IM, Stavrou I, Hoeffberger R, Szomolanyi P, Karanikas G, et al. High-resolution contrast-enhanced susceptibility-weighted MR imaging at 3T in patients with brain tumors: correlation with positron-emission tomography and histopathologic findings. *AJNR Am J Neuroradiol* 2007;28(7):1280-6.
8. Franceschi AM, Moschos SJ, Anders CK, Glaubiger S, Collichio FA, Lee CB, et al. Use of Susceptibility-Weighted Imaging (SWI) in the Detection of Brain Hemorrhagic Metastases from Breast Cancer and Melanoma. *J Comput Assist Tomogr* 2016;40(5):803-5.
9. Hamilton R, Krauze M, Romkes M, Omolo B, Konstantinopoulos P, Reinhart T, et al. Pathologic and gene expression features of metastatic melanomas to the brain. *Cancer* 2013;119(15):2737-46.
10. Kondziolka D, Bernstein M, Resch L, Tator CH, Fleming JF, Vanderlinden RG, et al. Significance of hemorrhage into brain tumors: clinicopathological study. *J Neurosurg* 1987;67(6):852-7.
11. Robinson RJ, Bhuta S. Susceptibility-weighted imaging of the brain: current utility and potential applications. *J Neuroimaging* 2011;21(4):189-204.
12. Wen PY, Macdonald DR, Reardon DA, Cloughesy TF, Sorensen AG, Galanis E, et al. Updated response assessment criteria for high-grade gliomas: response assessment in neuro-oncology working group. *J Clin Oncol* 2010;28(11):1963-72.
13. Berberat J, Grobholz R, Boxheimer L, Rogers S, Remonda L, Roelcke U. Differentiation between calcification and hemorrhage in brain tumors using susceptibility-weighted imaging: a pilot study. *AJR Am J Roentgenol* 2014;202(4):847-50.
14. Zhang W, Ma XX, Ji YM, Kang XS, Li CF. Haemorrhage detection in brain metastases of lung cancer patients using magnetic resonance imaging. *J Int Med Res* 2009;37(4):1139-44.
15. Roelcke U, Boxheimer L, Fathi AR, Schwyzer L, Ortega M, Berberat J, et al. Cortical hemosiderin is associated with seizures in patients with newly diagnosed malignant brain tumors. *J Neurooncol* 2013;115(3):463-8.
16. Park MJ, Kim HS, Jahng GH, Ryu CW, Park SM, Kim SY. Semiquantitative assessment of intratumoral susceptibility signals using non-contrast-enhanced high-field high-resolution susceptibility-weighted imaging in patients with gliomas: comparison with MR perfusion imaging. *AJNR Am J Neuroradiol* 2009; 30(7):1402-8.